iScience

CellPress
OPEN ACCESS

Article

Autographiviridae phage HH109 uses capsular polysaccharide for infection of *Vibrio alginolyticus*

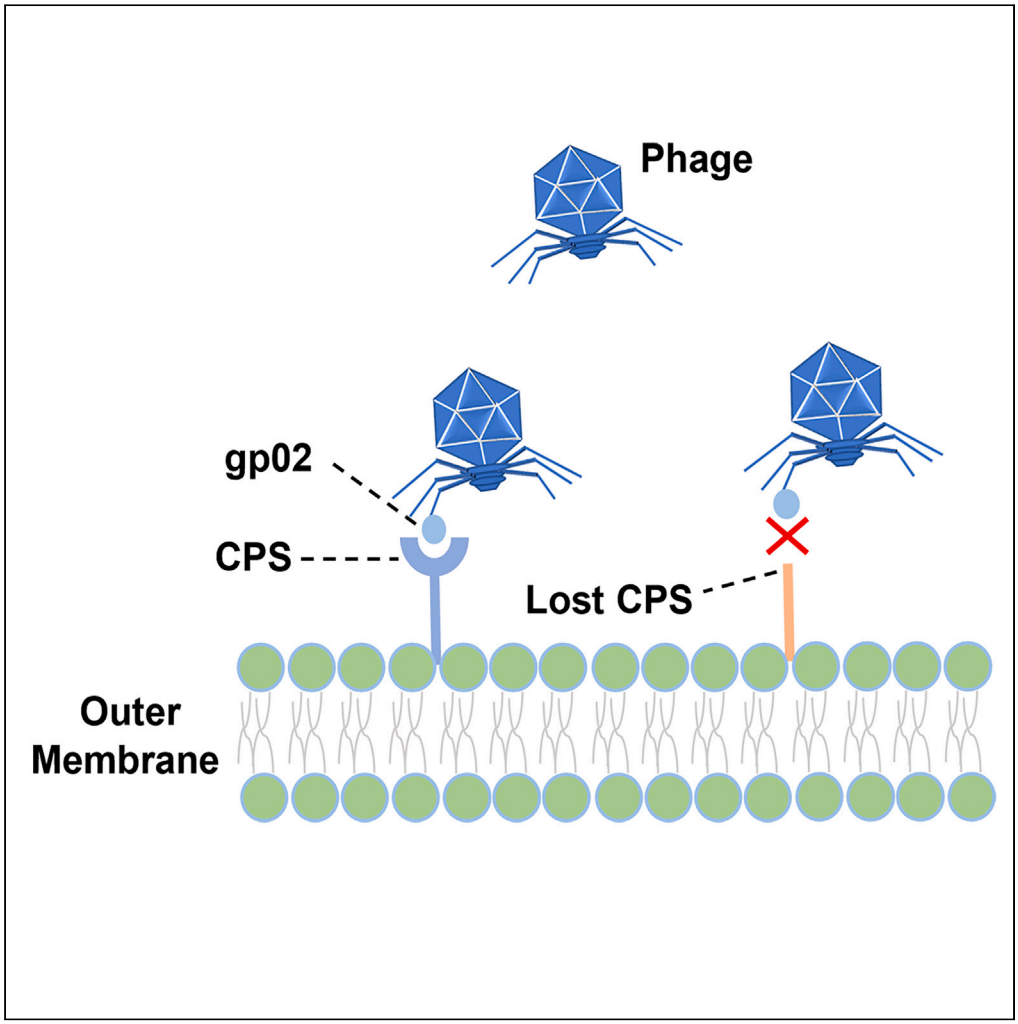

Xixi Li, Shenao Li, Chen Zhang, Ce Zhang, Xuefeng Xu, Xiaohui Zhou, Zhe Zhao

zhezhao@hhu.edu.cn

Highlights

Capsular polysaccharide (CPS) of E110 serves as the receptor for the phage HH109

Phage-resistant mutants mutate in genes responsible for CPS biosynthesis

The tail protein gp02 of phage HH109 recognizes and degrades host CPS

Li et al., iScience *27*, 110695
September 20, 2024
https://doi.org/10.1016/j.isci.2024.110695

iScience

CellPress
OPEN ACCESS

Article

Autographiviridae phage HH109 uses capsular polysaccharide for infection of *Vibrio alginolyticus*

Xixi Li,[1] Shenao Li,[1] Chen Zhang,[1] Ce Zhang,[1] Xuefeng Xu,[1] Xiaohui Zhou,[2] and Zhe Zhao[1,3,*]

SUMMARY

***Autographiviridae* phage HH109 is a lytic *Vibrio alginolyticus* E110-specific phage, but the molecular mechanism underlying host recognition of this phage remains unknown. In this study, a transposon mutagenesis library of E110 was used to show that several capsular polysaccharide (CPS) synthesis-related genes were linked to the phage HH109 infection. Gene deletion combined with multiple functional assays demonstrated that CPS serves as the receptor for the phage HH109. Deletions of CPS genes caused reduction or loss of capsule and reduced adsorption. Comparative genome analysis revealed that phage-resistant mutants harbored loss-of-function mutations in the previously identified genes responsible for CPS biosynthesis. The tail protein gp02 of phage HH109 was identified as the receptor-binding protein (RBP) on CPS using antibody blocking assay, immunofluorescence staining, and CPS quantification. Additionally, we found that the phage HH109 could degrade approximately 88% of mature biofilms. Our research findings provide a theoretical basis against vibriosis.**

INTRODUCTION

Bacteriophages (phages), the most abundant living entities on Earth, are recognized as critical components in food web ecology and major evolutionary drivers of bacterial communities.[1] Various components, including proteins to polysaccharides, have been identified in gram-negative bacteria as phage host receptors, such as capsular polysaccharides (CPS).[2] Capsules are surface polysaccharide structures that provide protective roles from physical and chemical stresses for many bacteria and also are essential for the virulence of pathogenic bacteria.[3] CPS made up of repeating linear or branched oligosaccharide units by joining linkages is highly diverse and has been used as a bacterial strain classification. Phages use CPS as receptors as well.[4] For example, *Stephanstirmvirinae* phage PNJ1809-36 reversibly binds to CPS for the initial adsorption, then irreversibly the host's second receptor LPS.[5] It was also reported that *Ackermannviridae* phage ΦCO01 adsorption to the host *Acinetobacter baumannii* requires the presence of an intact CPS.[6] It is worth noting that only a limited number of *Autographiviridae* phages, such as *Klebsiella pneumoniae* phage KP32 and *Escherichia coli* phage K1-5 have been identified as possessing receptor-binding proteins that specifically recognize CPS.[7,8]

Phage encoded receptor-binding proteins (RBPs) are key factors determining host range, mediating initial contact with host cell surface receptors. For example, in *Autographiviridae* phage KP32, tail tubular protein A is responsible for host-cell recognition, attachment, and initiation of infection.[7] The phage K1-5 encodes two distinct hydrolyzed tail fiber proteins for initial contact with their host receptors. One is the endosialidase protein, allowing the phage K1-5 to bind to and degrade K1 polysaccharide capsules. The other protein, nearly identical to the lyase, enables the phage to attach to and degrade K5 polysaccharide capsules.[8] Besides, *Autographiviridae* phage T7 possesses a lower nozzle encased by six or twelve tail fibers or tail spikes. The initial interaction of T7 with host membrane proteins facilitates further interaction between gp17 tail fibers and LPS. This interaction leads to a conformational change in the tail fibers, aligning them perpendicular to the cell surface and initiating protein and DNA ejection.[9,10] In summary, diverse phage groups use different mechanisms to interact with host cells due to their enormous structural diversity.

Vibrio species are ubiquitous and abundant in brackish water ecosystems worldwide, and some of them are zoonotic pathogens that can cause fatal diseases in aquatic animals and humans.[11,12] From a phage therapy point of view, many studies on *Vibrio*-specific phages have been widely reported, and phage receptors are also of concern. For example, *Vibrio* phage OWB utilizes the outer membrane protein (OMP) vp0980 as a receptor for adsorbing the host *V. parahaemolyticus*. In contrast, *Vibrio* phage VP3 employs TolC or LPS to adsorb the host *V. cholerae*[13,14] Additionally, *V. cholerae* phages vp882 and VP1 utilize the transcription factors VqmA and OMP PolyQ as a receptor, respectively.[15,16] Like OWB and VP1, phage KVP40 infects *V. anguillarum* using OMP as the host receptor.[17] Despite the presence of CPS on the surface of *Vibrio* species, there are few reports that CPS serves as a receptor for *Vibrio* phages.[18]

[1]Jiangsu Province Engineering Research Center for Marine Bio-resources Sustainable Utilization, College of Oceanography, Hohai University, Nanjing, Jiangsu, China
[2]School of Public Health and Emergency Management, Southern University of Science and Technology, Shenzhen, Guangdong, China
[3]Lead contact
*Correspondence: zhezhao@hhu.edu.cn
https://doi.org/10.1016/j.isci.2024.110695

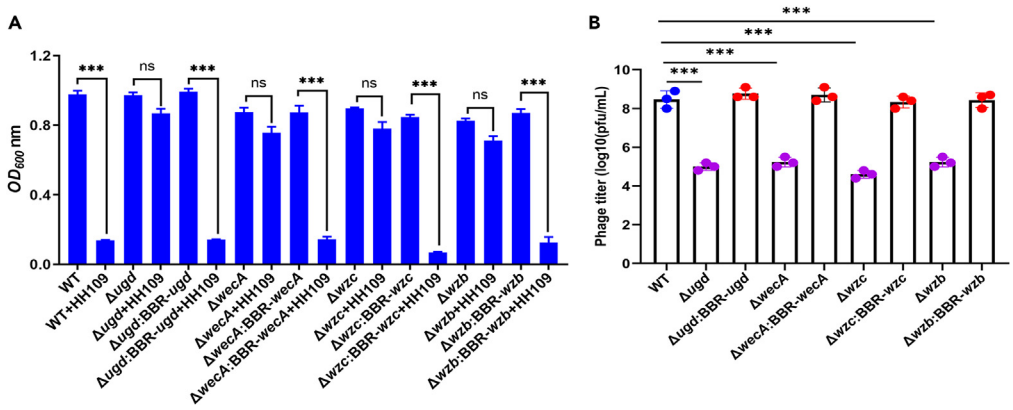

Figure 1. Several CPS genes of *V. alginolyticus* strain E110 are involved in the phage HH109 infection

(A) Growth assays of wild-type, deletion mutants, and complemented strains as indicated with or without the phage HH109 infection at 5 h.

(B) Phage titer assays in wild type, deletion mutants, and complemented strains. Data are displayed as the means ± SD from three independent experiments. Ns > 0.05, ***, $p < 0.0001$.

In our previous work, *Autographiviridae* phage HH109 could exclusively infect and efficiently lyse host strain *V. alginolyticus* E110. However, the mechanism of host recognition by phage HH109 to host E110 remains unknown. In this study, we identified CPS as the receptor of phage HH109 and the phage tail protein that binds to CPS was also confirmed. Additionally, we confirmed the destructive impact of phage HH109 on the mature biofilm of host E110. In summary, our work will be necessary for understanding the mechanisms of early interaction between *Vibrio* phages and pathogens and determining the application of phages in antimicrobial therapy.

RESULTS

Several CPS-related genes influence the phage HH109 infection

To identify host receptors of the phage HH109, we assembled a library of approximately 30,000 random transposon insertion mutants derived from *V. alginolyticus* E110. Eleven mutants were selected as phage-resistant upon initial screening and confirmed for significant reduction of lysis by monitoring the turbidity (OD_{600}) of the bacteria cultures in the presence of the phage and spot testing assays (Figures S1A and S1B). Transposon insertion sites determination by sequencing revealed that seven genes (*ugd*, *wecA*, *wzc*, *wzb*, *argE*, *JYG29_07705*, and *JYG29_22310*) were involved in transposon insertions in those eleven mutants, with two genes (*ugd* and *wecA*) represented in multiple mutants (Figure S1C). To further validate the screening data, we generated in-frame deletion mutants of seven genes and tested their effects on the phage HH109 infection. Bacterial growth and phage titer assays showed that individual deletion of the four genes, *ugd*, *wecA*, *wzc*, and *wzb* were not lysed, and phage titer decreased (Figures 1A and 1B). In contrast, complementation of those genes restored the phenotype of the wild-type strain (Figure 1). However, deletions of *JYG29_22310*, *argE*, and *JYG29_07705* did not affect bacterial lysis caused by the phage HH109 infection (Figure S1D), which was inconsistent with the result of transposon insertion, indicating that polar effect occurred due to transposon insertion. Notably, the four genes (*ugd*, *wecA*, *wzc*, and *wzb*) are all annotated to be related to CPS biosynthesis (Figure S1C); however, *wzc* and *wzb* are not located within the CPS synthesis gene cluster. These data indicated bacterial CPS may be necessary for the phage HH109 infection.

V. alginolyticus CPS serves as the receptor for the phage HH109 adsorption

To further elucidate whether CPS is involved in the phage HH109 infection, we identified the entire CPS gene cluster from *V. alginolyticus* E110 based on whole-genome sequencing (GenBank: PRJNA842900). The remaining thirty-four genes within the CPS loci, except *ugd* and *wecA*, were then individually or tandemly deleted. The susceptibility of those mutants to the phage was evaluated based on bacterial growth and phage spot testing assays. The results showed that deletions of *gt1*, *gt6*, and *orf2* made the bacterial cells resistant to the phage HH109 infection, while *in trans* expression of *gt1*, *gt6*, and *orf2* in their deletion mutants restored the susceptibility (Figures 2A and S2C). By comparison, disruption of other genes did not impact phage infection (Figures S2A and S2B). The *gt1* and *gt6* encode glycosyltransferase, and the *orf2* encodes an ATP-grasp fold amidoligase family protein. To address why only some of the CPS genes were important for phage HH109 infection, we further analyzed the capsules of both phage-resistant and phage-sensitive mutants using qualitative and quantitative methods. Take *ugd* as an example, capsule staining showed that the wild-type and complemented strains (Δ*ugd*: BBR-*ugd*) exhibited a halo surrounding a cell, indicating the presence of capsules in the peripheral part; on the contrary, the Δ*ugd* mutant did not show any halo (Figure 2B, upper panel); Meanwhile, scanning electron microscopy (SEM) observation also revealed that the surface of the wild-type and complemented strains was rough whereas the Δ*ugd* mutant was smooth (Figure 2B, upper panel). Similar phenotypes were also observed in the *wecA*, *gt1*, *gt6*, and *orf2* deletion mutants (Figure S3A). As a control, the Δ*galU* and Δ*mbL* mutants that remained sensitive to the phage infection were randomly selected for capsule staining and SEM observation, and the data showed the two strains have identical phenotypes to the wild-type strain

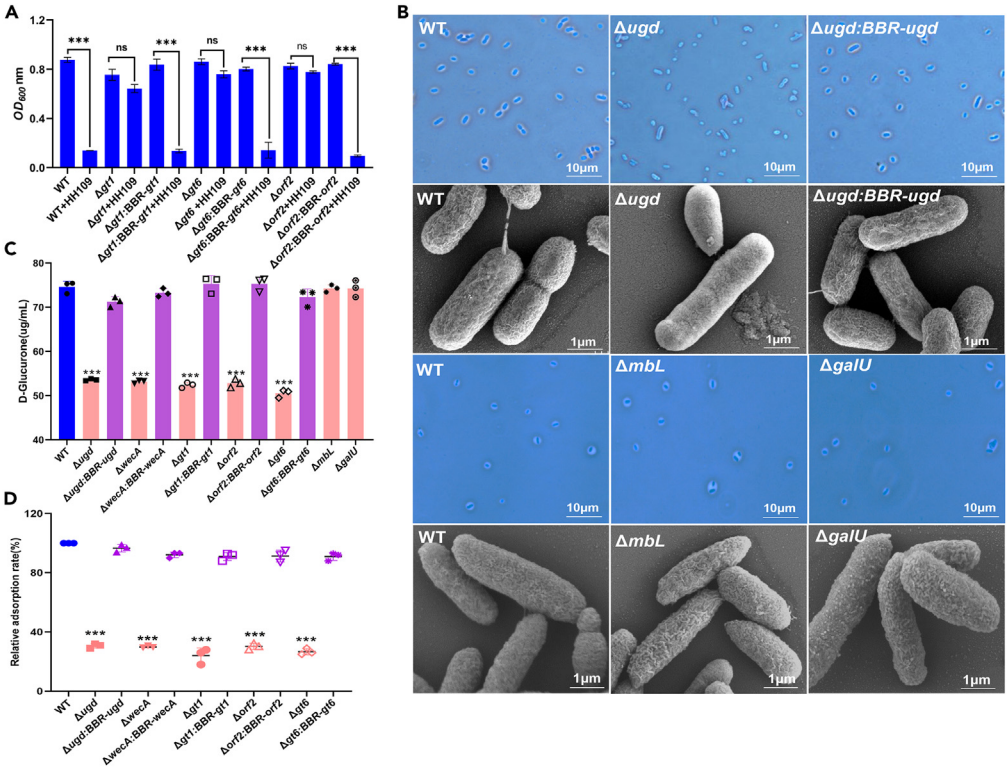

Figure 2. CPS in *V. alginolyticus* strain E110 functions as the receptor for the phage HH109 adsorption

(A) Growth assays of wild type, deletion mutants, and complemented strains as indicated with or without the phage HH109 infection at 5 h.

(B) Cell morphology observation of different strains by light microscopy after capsule staining or scanning electron microscopy. The halo surrounding the cells indicates the presence of capsules. Strain names labeled on the top left corner of each picture.

(C) Quantitative assay of CPS. Surface capsular polysaccharides produced by each strain as indicated were measured and compared with the wild-type strain.

(D) Phage adsorption assays. The number of phages that remained in the supernatant was determined after 10 min adsorption of the phage HH109 on the wild type, deletion mutants, and complemented strains as indicated. Data are displayed as the means ± SD from three independent experiments. Ns > 0.05, ***, $p < 0.0001$.

(Figure 2B, lower panel). Furthermore, the quantitative analysis also confirmed that the five mutants (Δ*ugd*, Δ*wecA*, Δ*gt1*, Δ*orf2*, and Δ*gt6*) yielded much lower CPS contents than the wild-type, Δ*mbL*, and Δ*galU* strains (Figure 2C). Taken together, these results indicated that the deletions of *ugd*, *wecA*, *gt1*, *gt6*, and *orf2* significantly reduced CPS yield of *V. alginolyticus* E110 and in consequence caused diminishing susceptibility to the phage HH109. In contrast, the deletions of the remaining within the CPS loci barely changed the CPS amount.

Capsule constitutes the outmost layer of bacterial cells; therefore, we assume that the CPS of *V. alginolyticus* E110 is the receptor for phage infection. Consequently, we measured the adsorption rate of the phage HH109 on different deletion mutants. As expected, deletions of *ugd*, *wecA*, *gt1*, *orf2*, and *gt6* caused a significant reduction in the phage adsorption compared with their corresponding complemented and wild-type strains (Figure 2D). Using a diverse set of mutants (Δ*lpxM*, Δ*waaF*, Δ*waaA*, Δ*hldE*, Δ*rfbB*, and Δ*rfbA*) in the lipopolysaccharide (LPS) locus, we demonstrated that LPS is not essential for phage HH109 adsorption (Figure S3B). Similarly, phage HH109 does not use a protein receptor as proteinase K treatment of cells did not prevent phage binding (Figure S3C). Therefore, we suggest that phage HH109 uses the CPS of *V. alginolyticus* E110 as a receptor for adsorption.

The phage HH109 predation drove the rapid emergence of phage-resistant *V. alginolyticus* through the reduction or loss of CPS

Although the phage HH109 causes rapid lysis of strain E110, we noticed regrowth of HH109 infected cultures after 6 h of incubation (Figure 3A). The phenomenon was supported by the spot plate assays after overnight incubation (Figure 3B), indicating the development of spontaneous phage-resistant mutants. Five colonies were picked, and their phage-resistant phenotypes were confirmed (Figures S4A and S4B). In addition, they displaced deficient CPS production (Figure 3C). As a result, the phage HH109 was unable to efficiently adsorb to their cell surface compared with the wild type (Figure 3D). Subsequently, we carried out a comparative genome analysis between the five phage-resistant isolates and the wild-type strain, showing that four resistant isolates all harbored mutations of single nucleotide substitution (EP1 and EP3), or a 10-bp deletion (EP2), or 19-bp insertion (EP4) in the coding region of *wecA*. At the same time, EP5 had a single nucleotide substitution in the coding region of *orf2* (Figure 3E). Thus, our data indicate that phage resistance phenotype in the late stage of HH109 infection arose through

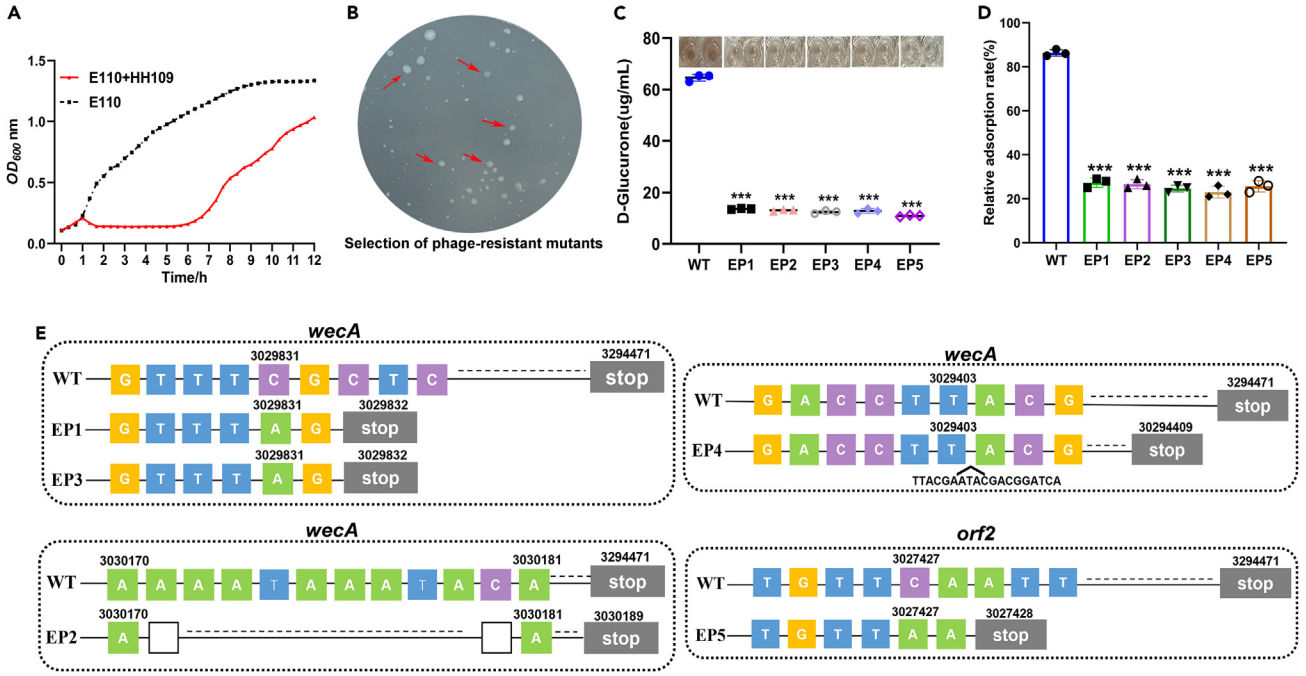

Figure 3. Mechanism for the emergence of phage-resistant *V. alginolyticus* isolates under the pressure of the phage HH109 infection

(A) Growth curves of *V. alginolyticus* strain E110 with or without the phage HH109 infection over a 12 h time course.

(B) Spot plate assay of strain E110 with the phage HH109 showed the emergence of some bacterial colonies within the large central lysis zone (red arrowheads) at overnight incubation.

(C) Quantitative assay of CPS. Surface capsular polysaccharides produced by five phage-resistant isolates (EP1, EP2, EP3, EP4, and EP5) were measured and compared with those in the wild-type strains.

(D) Phage adsorption assays. The number of phages in the supernatant was determined after 10 min adsorption of the phage HH109 on EP1, EP2, EP3, EP4, EP5, and WT. ***, $p < 0.0001$.

(E) Mutations in the five phage-resistant isolates derived from *V. alginolyticus* strain E110. EP1, EP2, EP3, and EP4 all have mutations in the coding region of *wecA* by substitution, deletion or insertion, while EP5 has a single nucleotide substitution in the coding region of *orf2*. Numbers represent gene nucleotide positions, and box colors represent different nucleotides. Blank, deletion; Caret, insertion; gray, stop codon.

the reduction or loss of CPS receptor that caused by gene frameshift in *wecA* and *orf2*. These findings further confirmed that the CPS of the E110 strain is an adsorption receptor of phage HH109 and suggested that the capsule receptors are prone to change by a genetic mutation to develop resistance to phage infection.

Phage gp02 binds to CPS of host cells

To identify RBPs of the phage HH109, Interpro (https://www.ebi.ac.uk/interpro/) was utilized to predict the structural domains of phage tail-associated proteins. The tail fiber protein gp02 was identified in the genome since it harbored a pectin_lyase_fold/virulence homologous superfamily, and the domain is essential for the phage KP32 spike proteins gp37 and gp38 (Figure 4A), which acted as a depolymerase to degrade *Klebsiella pneumoniae* capsular polysaccharide via spot testing.[19] The protein structure of gp02 was predicted by AlphaFold2, which overlaps with the structure of phage KP32 spike protein gp38, further supporting the annotation of gp02 protein as a spike protein (Figure S5). Therefore, we constructed and purified the recombinant protein gp02 (fused with His and TF tag) and generated anti-serum against the gp02. We found that when the phage HH109 was pretreated with the anti-gp02 serum, the titer of free phages went down by roughly 65% compared with the regular serum-pretreated and untreated group (Figure 4B), and protein competition assay revealed that the phage adsorption was reduced by about 60% after gp02 was blocked by the phage HH109 (Figure 4C), indicating that gp02 is the RBP. Notably, the binding of the gp02 to host CPS was observed by immunofluorescence staining (Figure 4D), showing that the wild-type strain, not the *ugd* deletion mutant, was labeled by the HIS-tag antibody (red fluorescence) after they were pre-incubated with the recombinant protein gp02. The wild-type strain was not labeled as a negative control after pre-incubating with the tag protein trigger factor (TF). These findings suggested that the gp02 directly interacts with the host receptor CPS and mediates HH109 infection. To make sure whether the gp02 has polysaccharide depolymerase activity, we quantified the CPS contents of different strains, showing that the content of E110 strain after gp02-treated was similar to that of Δ*ugd* but significantly lower than those of E110 after TF-treated or untreated (Figure 4E); meanwhile, an examination of those strains after capsular staining also revealed disappear of the halo around gp02-treated cells (Figure 4F), indicating that the gp02 can depolymerize CPS of E110. Furthermore, the conclusion was supported by SDS-PAGE analysis that CPS degradation required the gp02 in a

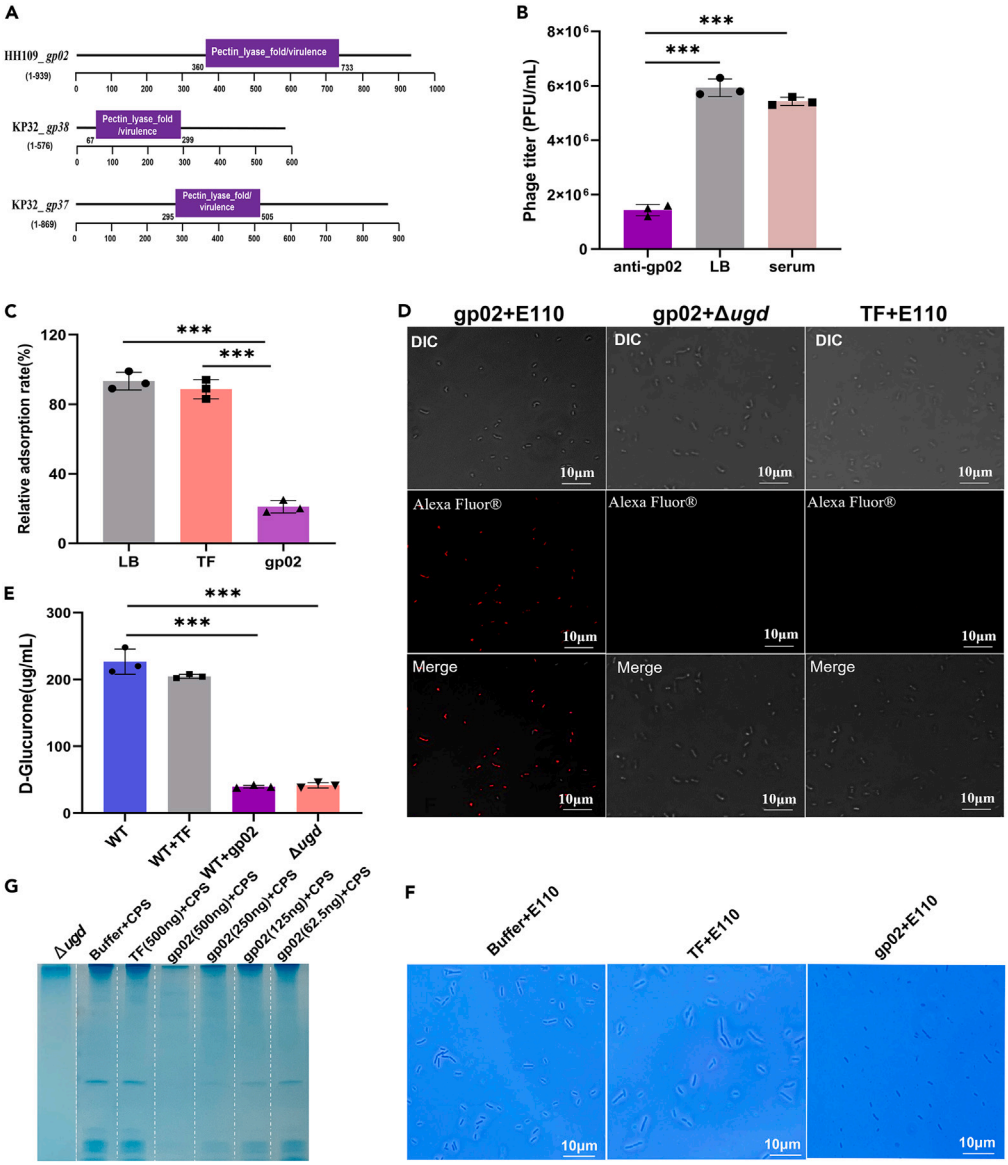

Figure 4. GP02 acts as RBP to recognize the CPS in *V. alginolyticus* strain E110

(A) Schematic diagram of phage tail proteins gp02, gp37, and gp38. Gp02, a phage HH109 tail protein, includes a pectin lyase fold/virulence (360–733) homologous superfamily. gp37 and gp38 are both from *Klebsiella* phage KP32 and have the Pectin lyase fold/virulence homologous superfamily (located in 295–505 and 67–299, respectively).

(B) Antibody blocking assay. Anti-gp02 serum was mixed with the phage HH109 for 10 min at RT and then added into the *V. alginolyticus* strains E110 for 1 h to assess phage titer. The normal serum was used as a control. The phage titer in the supernatant was determined. Data are displayed as the means ± SD from three independent experiments, and significance was determined by a Student's t test. ***, $p \leq 0.0001$.

(C) Protein competition assay in phage adsorption. *V. alginolyticus* strain E110 was pre-incubated with the recombinant protein gp02 (with tag TF) or the Tag TF for 10 min and then added into the phage HH109 to evaluate the phage adsorption rate. LB group (without protein pre-incubation) was used as a control, and the adsorption rate was set at 100%. Data are displayed as the means ± SD from three independent experiments, and significance was determined by a Student's t test. ***, $p \leq 0.0001$.

(D) Immunofluorescence assay showing the binding of GP02 to CPS of *V. alginolyticus* strain E110. Strains E110 and Δ*ugd* were pre-incubated with the recombinant protein GP02 (with tag TF) for 30 min and then subjected to an immunofluorescence assay using the HIS antibody as the primary antibody and the Alexa Fluor 594 goat anti-rabbit IgG as second antibody. As a control, the tag protein TF was also included to pre-incubate with strain E110. All samples were examined under a fluorescence microscope at 100×magnification, and red fluorescence indicates the presence of the recombinant protein GP02.

(E) Quantitative assay of CPS. CPS was extracted from *V. alginolyticus* strain E110 after incubation with the recombinant protein GP02 (with tag TF) or the tagger protein TF and quantified by measuring the concentration of uronic acid. The deletion mutant Δ*ugd* was included as a negative control. Data are displayed as the means ± SD from three independent experiments. ***, $p < 0.0001$.

Figure 4. *Continued*

(F) CPS staining and observation. *V. alginolyticus* strain E110 was incubated with the recombinant protein GP02 (with tag TF) or the tag protein TF and then visualized under light microscopy after capsule staining.

(G) CPS degradation in the dose-dependent effect of GP02. CPS was extracted from *V. alginolyticus* strain E110 and then incubated with 2-fold serial dilutions of the recombinant protein GP02 (with tag TF) or the tag protein TF. All samples were subjected to SDS-PAGE analysis and alcian blue staining.

dose-dependent manner when the purified gp02 and the extracted CPS were incubated together *in vitro* (Figure 4G). In summary, we concluded that the phage HH109 uses the tail spike gp02 to recognize and degrade host CPS to facilitate infection specifically.

Phage HH109 causes the dispersion of mature biofilm of *V. alginolyticus*

To explore the therapeutic potential of phage HH109 in disturbing *V. alginolyticus* biofilms, we investigated the dynamic process of biofilm formation by *V. alginolyticus*. Crystal violet staining assays showed that the biofilm of *V. alginolyticus* E110 reached its highest growth value at 12–20 h with mature biofilm (Figure 5A). Subsequently, the mature biofilm of E110 strain was exposed to the phage HH109 diluted by a 10-fold gradient. As shown in Figure 5B, biofilm was significantly dispersed by phage HH109 at different concentrations (1.2×10^9, 1.2×10^8, and 1.2×10^7 pfu/mL); after 8 h, phage HH109 degraded 88%, 64%, and 45% of the biofilm biomass at concentrations 1.2×10^9, 1.2×10^8, and 1.2×10^7 pfu/mL respectively, when compared to control (no phage). The aforementioned results indicate that the *Vibrio* phage HH109 could act as a potential biocontrol agent.

DISCUSSION

Adsorption is the first step in phage infection and is one of the critical factors responsible for determining host range. The successful attachment of phages to the host surface depends on their host receptors and RBPs. The host receptor utilized by phages can be any component of the bacterial surface, including CPS, LPS residues in gram-negative bacteria, flagella, pili, or outer membrane proteins.[2] Meanwhile, the RBPs of phages are usually named tail fibers, tail spikes, and tail tips. Here, we illustrate the mechanism by which HH109 recognizes host *V. alginolyticus* E110, which has been rarely reported in *Vibrio*.

Mutation analysis demonstrates that five genes involved in the CPS synthesis of *V. alginolyticus* have mutated, resulting in phage resistance. Deletion of glycosyltransferases (gt1 and gt2) may destroy glycosidic bonds in *V. alginolyticus* CPS leading to impaired synthesis of the CPS, which in turn affects the ability of phage HH109 to infect the host E110. These results were partially consistent with a previous study that found loss-of-function of *gt2* in the host, reducing the adsorption capacity of phage EFap02.[20] Deleting the gene *wecA* in *V. alginolyticus* abolishes the synthesis of GlcNAc, indispensable for phage HH109 adsorption and subsequent infection. Similarly, previous studies have shown that the inactivation of WecA results in the loss of polymer and "primer" consisting of undecaprenyl pyrophosphoryl (und-PP)-linked GlcNAc, inhibits the *Drexlerviridae* phage NJS1 adsorption to the O-antigen of host.[21] The hypothetical protein-encoding gene *orf2* is predicted to belong to the ATPgrasp_TupA protein family, which is involved in many different biological processes.[22] Thus, the lack of synthesis of transferase encoded by orf2 may affect the amidation of a downstream enzyme during the synthesis of *V. alginolyticus* CPS, resulting in impaired phage HH109. Deletion of the *ugd* gene prohibits the synthesis of UDP GlcA, the prominent component of CPS, preventing HH109 adsorption to host bacteria, and further biochemical experiments are needed to verify this assumption.

In addition to genes on the CPS loci of *V. alginolyticus* E110, the genes *wzb* and *wzc* located outside the CPS loci also regulate susceptibility to phage HH109 by disrupting capsule synthesis. Previous reports indicated that three consecutive genes, *wza*, *wzb*, and *wzc* constitute an essential exportation system in group 1 and 4 capsules in *E. coli*.[23] In the present study, it is worth explaining that genes *wza*, *wzb*, and *wzc* are sequentially located on chromosome II of E110. Therefore, we speculate that *wzb* and *wzc* deletion hindered the synthesis and export of CPS and further affected phage HH109 adsorption to the host. However, this gene *wza* has not yet been identified. The aforementioned studies indicate that the CPS of host *V. alginolyticus* is involved in the infection of phage HH109.

Bacteria can quickly adapt to external pressures and evolve strategies to circumvent phage infection.[24] For example, spontaneous phage-resistant strains of *V. cholerae* were found to delete 14 glutamine residues in the protein polyQ, resulting in phage VP1 resistance.[16] Meanwhile, *Acinetobacter baumannii* loses function mutations in genes responsible for capsule biosynthesis, resulting in capsule loss and disruption of *Ackermannviridae* phage ΦCO01 adsorption.[6] Similarly, our results found that the CPS biosynthesis genes *wecA* and *orf2* underwent frameshift, reducing the adsorption of phage HH109. Thus, we attribute the emergence of phage HH109 resistance to the loss of *V. alginolyticus*'s capsule.

The tailed phages typically use tail spikes or tail fiber proteins to recognize the bacterial surface at the early stage of infection by specifically digesting the polysaccharides, the primary receptors for phages.[25,26] For example, the *Autographiviridae* phage T7 uses tail fiber gp17 interactions with the surface polysaccharide LPS of *E. coli* at the initial adsorption. Unlike T7, *Autographiviridae* phage K1-5 adsorbs the CPS receptor using the tail spike.[2] Here, we found that tail protein gp02, predicted to encode a depolymerase in the phage HH109 tail, was the RBP interacting with the CPS of E110.

Biofilms cause most bacterial infections and conventional antibiotics cannot penetrate biofilms; therefore, they are ineffective in treating biofilm-related infections.[27] Previous studies reported the potential of phages and their derivatives have anti-biofilm potential against *Vibrio*.[28,29] In this study, phage HH109 exhibited a strong ability to disrupt biofilms, which is consistent with the report by Gao et al.[30] However, Yin et al.'s report indicated that the phage is expected to prevent biofilm formation but will not destroy the biofilm that has already formed.[31] The aforementioned evidence suggests that *Vibrio* phage HH109 could act as a potential biocontrol agent.

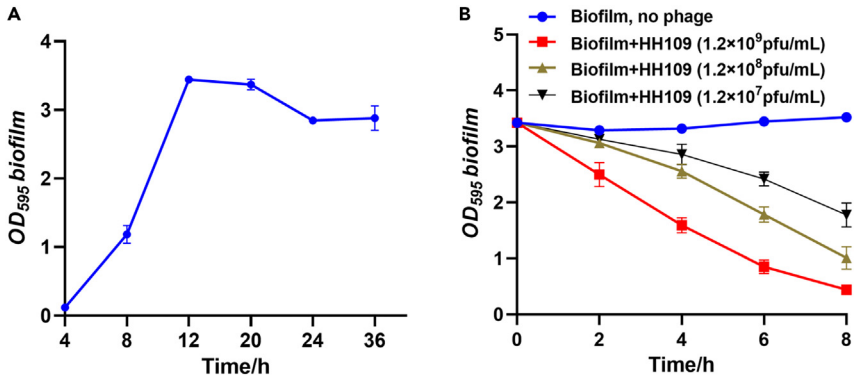

Figure 5. Degradation of *V. alginolyticus* biofilm by phage HH109

(A) Biofilm-forming capacity of *V. alginolyticus* E110. Bacterial overnight cultures were diluted in fresh LB with 2% NaCl, transferred into a 24-well plate, and incubated at 30°C to allow biofilm formation. After 4, 8, 12, 20, 24, and 36 h, the biofilms were measured at OD_{595} nm.

(B) Degradation of mature biofilm by phage HH109. 1 mL phage (1.2×10^9, 1.2×10^8, and 1.2×10^7 pfu/mL) was added to a 24-well plate with mature biofilm; biofilm was measured after 2, 4, 6, and 8 h. Data represent the mean of at least five biological replicates ±SD, analyzed in three technical repetitions.

In summary, we elucidated that *Autographiviridae* phage HH109 utilizes the tail protein gp02 to recognize and degrade the host E110's CPS to initiate infection. Concurrently, we also confirmed that disrupting the CPS biosynthesis gene in E110 leads to the rapid development of phage-resistant strains. Moreover, the phage HH109 can disperse the biofilm of *V. alginolyticus* E110. Our research contributes to the understanding of the early interaction mechanism between *Autographiviridae* phages and pathogens but also serves as a crucial reference for the application of phages in biofilm eradication.

Limitations of the study

Although our study indicates that phage HH109 uses the tail protein gp02 to recognize the CPS of the host *V. alginolyticus* for initiating infection. We also observed that phage HH109 exhibits inefficient infection against CPS mutants. Further experiments are required to verify whether this phage utilizes other types of adsorption receptors.

STAR★METHODS

Detailed methods are provided in the online version of this paper and include the following:

- KEY RESOURCES TABLE
- RESOURCE AVAILABILITY
  - Lead contact
  - Materials availability
  - Data and code availability
- EXPERIMENTAL MODEL AND STUDY PARTICIPANT DETAILS
- METHOD DETAILS
  - Bacterial strains, plasmids, and growth conditions
  - Transposon mutagenesis and screening of phage-resistant mutants
  - Transposon insertion site determination
  - Gene knockout and complementation
  - Lysis curve determination and spot testing assays
  - Phage adsorption assay
  - Microscopy observation on the bacterial capsule
  - Capsule extraction and quantification
  - Identification of the phage receptor type
  - Isolation of phage-resistant *V. alginolyticus* mutants
  - Genome sequencing and comparative analysis
  - Protein expression, purification, and anti-serum preparation
  - Antibody blocking and protein competition assay
  - Immunofluorescence analysis
  - Assays on degradation activity of purified gp02
  - Assay of biofilm-dispersing activity

- QUANTIFICATION AND STATISTICAL ANALYSIS
- ADDITIONAL RESOURCES

SUPPLEMENTAL INFORMATION

Supplemental information can be found online at https://doi.org/10.1016/j.isci.2024.110695.

ACKNOWLEDGMENTS

We thank Prof. Weiqin Li and Haibin Hao from the Affiliated Jinling Hospital of Nanjing University School of Medicine for their support in extracting capsular polysaccharides (Chinese patent no. ZL202211527380.5); we thank Gene Denovo (Guangzhou, China) for providing the sequencing platform and bioinformation analysis; we would like to congratulate Aibotech Biotechnology co., Ltd (Wuhan, China) for providing gp02 antibody preparation and Beijing Qingxi technology research institute (Beijing, China) for providing CPS purification and structure elucidation services.

This work was partially supported by the National Natural Science Foundation of China (31872597), Jiangsu Agricultural Science and Technology Independent Innovation Fund (CX [23]1007), Fundamental Research Funds for the Central Universities (B220203038), Postgraduate Research & Practice Innovation Program of Jiangsu Province (42200333), Guangdong Basic and Applied Basic Research Foundation (2023B1515120016), Shenzhen Science and Technology Innovation Commission (JCYJ20220818100616034), Shenzhen Medical Research Fund (B2302024).

AUTHOR CONTRIBUTIONS

X.L: conceptualization, methodology, validation, formal analysis, and writing – original draft; S.L, Chen Z., Ce Z., and X.X: methodology, formal analysis; X.Z.: conceptualization, methodology, review and editing; Z.Z.: conceptualization, formal analysis, writing – original draft, writing – review and editing, resources, supervision, funding acquisition.

DECLARATION OF INTERESTS

The authors declare no competing interests.

Received: April 10, 2024
Revised: May 21, 2024
Accepted: August 6, 2024
Published: August 8, 2024

REFERENCES

1. Dion, M.B., Oechslin, F., and Moineau, S. (2020). Phage diversity, genomics and phylogeny. Nat. Rev. Microbiol. *18*, 125–138.
2. Nobrega, F.L., Vlot, M., de Jonge, P.A., Dreesens, L.L., Beaumont, H.J.E., Lavigne, R., Dutilh, B.E., and Brouns, S.J.J. (2018). Targeting mechanisms of tailed bacteriophages. Nat. Rev. Microbiol. *16*, 760–773.
3. Liston, S.D., Ovchinnikova, O.G., and Whitfield, C. (2016). Unique lipid anchor attaches Vi antigen capsule to the surface of *Salmonella enterica* serovar Typhi. Proc. Natl. Acad. Sci. USA *113*, 6719–6724.
4. Kenyon, J.J., Marzaioli, A.M., Hall, R.M., and De Castro, C. (2015). Structure of the K12 capsule containing 5,7-di-N-acetylacinetaminic acid from *Acinetobacter baumannii* isolate D36. Glycobiology *25*, 881–887.
5. Gong, Q., Wang, X., Huang, H., Sun, Y., Qian, X., Xue, F., Ren, J., Dai, J., and Tang, F. (2021). Novel Host Recognition Mechanism of the K1 Capsule-Specific Phage of *Escherichia coli*: Capsular Polysaccharide as the First Receptor and Lipopolysaccharide as the Secondary Receptor. J. Virol. *95*, e0092021.
6. Gordillo Altamirano, F., Forsyth, J.H., Patwa, R., Kostoulias, X., Trim, M., Subedi, D., Archer, S.K., Morris, F.C., Oliveira, C., Kielty, L., et al. (2021). Bacteriophage-resistant *Acinetobacter baumannii* are resensitized to antimicrobials. Nat. Microbiol. *6*, 157–161.
7. Pyra, A., Brzozowska, E., Pawlik, K., Gamian, A., Dauter, M., and Dauter, Z. (2017). Tail tubular protein A: a dual-function tail protein of *Klebsiella pneumoniae* bacteriophage KP32. Sci. Rep. *7*, 2223.
8. Scholl, D., Rogers, S., Adhya, S., and Merril, C.R. (2001). Bacteriophage K1-5 encodes two different tail fiber proteins, allowing it to infect and replicate on both K1 and K5 strains of *Escherichia coli*. J. Virol. *75*, 2509–2515.
9. Arnaud, C.A., Effantin, G., Vivès, C., Engilberge, S., Bacia, M., Boulanger, P., Girard, E., Schoehn, G., and Breyton, C. (2017). Bacteriophage T5 tail tube structure suggests a trigger mechanism for *Siphoviridae* DNA ejection. Nat. Commun. *8*, 1953.
10. González-García, V.A., Pulido-Cid, M., Garcia-Doval, C., Bocanegra, R., van Raaij, M.J., Martín-Benito, J., Cuervo, A., and Carrascosa, J.L. (2015). Conformational changes leading to T7 DNA delivery upon interaction with the bacterial receptor. J. Biol. Chem. *290*, 10038–10044.
11. Baker-Austin, C., Oliver, J.D., Alam, M., Ali, A., Waldor, M.K., Qadri, F., and Martinez-Urtaza, J. (2018). *Vibrio spp.* infections. Nat. Rev Dis. Primers *4*, 1–19.
12. Austin, B. (2010). Vibrios as causal agents of zoonoses. Vet. Microbiol. *140*, 310–317.
13. Hu, M., Zhang, H., Gu, D., Ma, Y., and Zhou, X. (2020). Identification of a novel bacterial receptor that binds tail tubular proteins and mediates phage infection of *Vibrio parahaemolyticus*. Emerg. Microbes Infect. *9*, 855–867.
14. Fan, F., Li, X., Pang, B., Zhang, C., Li, Z., Zhang, L., Li, J., Zhang, J., Yan, M., Liang, W., and Kan, B. (2018). The outer-membrane protein TolC of *Vibrio cholerae* serves as a second cell-surface receptor for the VP3 phage. J. Biol. Chem. *293*, 4000–4013.
15. Duddy, O.P., Huang, X., Silpe, J.E., and Bassler, B.L. (2021). Mechanism underlying the DNA-binding preferences of the *Vibrio cholerae* and vibriophage VP882 VqmA quorum-sensing receptors. PLoS Genet. *17*, e1009550.
16. Fan, F., Li, Z., Wang, J., Diao, B., Liang, W., and Kan, B. (2021). A PolyQ Membrane Protein of *Vibrio cholerae* Acts as the Receptor for Phage Infection. J. Virol. *95*, e02245-20.
17. Castillo, D., Rørbo, N., Jørgensen, J., Lange, J., Tan, D., Kalatzis, P.G., Svenningsen, S.L., and Middelboe, M. (2019). Phage defense mechanisms and their genomic and phenotypic implications in the fish pathogen *Vibrio anguillarum*. FEMS Microbiol. Ecol. *95*, 1–13.
18. Albert, M.J., Bhuiyan, N.A., Rahman, A., Ghosh, A.N., Hultenby, K., Weintraub, A.,

Nahar, S., Kibriya, A.K., Ansaruzzaman, M., and Shimada, T. (1996). Phage specific for *Vibrio cholerae* O139 Bengal. J. Clin. Microbiol. *34*, 1843–1845.
19. Majkowska-Skrobek, G., Latka, A., Berisio, R., Squeglia, F., Maciejewska, B., Briers, Y., and Drulis-Kawa, Z. (2018). Phage-Borne Depolymerases Decrease *Klebsiella pneumoniae* Resistance to Innate Defense Mechanisms. Front. Microbiol. *9*, 2517.
20. Liu, J., Zhu, Y., Li, Y., Lu, Y., Xiong, K., Zhong, Q., and Wang, J. (2022). Bacteriophage-Resistant Mutant of *Enterococcus faecalis* Is Impaired in Biofilm Formation. Front. Microbiol. *13*, 913023.
21. Hao, G., Yuan, C., Shu, R., Jia, Y., Zhao, S., Xie, S., Liu, M., Zhou, H., Sun, S., and Wang, H. (2021). O-antigen serves as a two-faced host factor for bacteriophage NJS1 infecting nonmucoid *Klebsiella pneumoniae*. Microb. Pathog. *155*, 104897.
22. Ogasawara, Y., and Dairi, T. (2017). Biosynthesis of Oligopeptides Using ATP-Grasp Enzymes. Chemistry *23*, 10714–10724.
23. Whitfield, C. (2006). Biosynthesis and assembly of capsular polysaccharides in *Escherichia coli*. Annu. Rev. Biochem. *75*, 39–68.
24. Oechslin, F. (2018). Resistance Development to Bacteriophages Occurring during Bacteriophage Therapy. Viruses *10*, 351.
25. Yan, J., Mao, J., and Xie, J. (2014). Bacteriophage polysaccharide depolymerases and biomedical applications. BioDrugs *28*, 265–274.
26. Li, X., Koç, C., Kühner, P., Stierhof, Y.D., Krismer, B., Enright, M.C., Penadés, J.R., Wolz, C., Stehle, T., Cambillau, C., et al. (2016). An essential role for the baseplate protein Gp45 in phage adsorption to *Staphylococcus aureus*. Sci. Rep. *6*, 26455.
27. Ma, Z., Han, J., Chang, B., Gao, L., Lu, Z., Lu, F., Zhao, H., Zhang, C., and Bie, X. (2017). Membrane-Active Amphipathic Peptide WRL3 with in Vitro Antibiofilm Capability and in Vivo Efficacy in Treating Methicillin-Resistant Staphylococcus aureus Burn Wound Infections. ACS Infect. Dis. *3*, 820–832.
28. Kim, S.G., Jun, J.W., Giri, S.S., Yun, S., Kim, H.J., Kim, S.W., Kang, J.W., Han, S.J., Jeong, D., and Park, S.C. (2019). Isolation and characterisation of pVa-21, a giant bacteriophage with anti-biofilm potential against Vibrio alginolyticus. Sci. Rep. *9*, 6284.
29. Srinivasan, R., Chaitanyakumar, A., Subramanian, P., Mageswari, A., Gomathi, A., Aswini, V., Sankar, A.M., Ramya, M., and Gothandam, K.M. (2020). Recombinant engineered phage-derived enzybiotic in Pichia pastoris X-33 as whole cell biocatalyst for effective biocontrol of *Vibrio parahaemolyticus* in aquaculture. Int. J. Biol. Macromol. *154*, 1576–1585.
30. Gao, L., Ouyang, M., Li, Y., Zhang, H., Zheng, X.F., Li, H.X., Rao, S.Q., Yang, Z.Q., and Gao, S. (2022). Isolation and Characterization of a Lytic Vibriophage OY1 and Its Biocontrol Effects Against *Vibrio spp*. Front. Microbiol. *13*, 830692.
31. Yin, Y., Ni, P., Liu, D., Yang, S., Almeida, A., Guo, Q., Zhang, Z., Deng, L., and Wang, D. (2019). Bacteriophage potential against *Vibrio parahaemolyticus* biofilms. Food Control *98*, 156–163.
32. Nguyen, A.N., Disconzi, E., Charrière, G.M., Destoumieux-Garzón, D., and Bouloc, P. (2018). csrB Gene Duplication Drives the Evolution of Redundant Regulatory Pathways Controlling Expression of the Major Toxic Secreted Metalloproteases in Vibrio tasmaniensis LGP32. mSphere *3*, 10.
33. Milton, D.L., Norqvist, A., and Wolf-Watz, H. (1992). Cloning of a metalloprotease gene involved in the virulence mechanism of *Vibrio anguillarum*. J. Bacteriol. *174*, 7235–7244.
34. Val, M.E., Skovgaard, O., Ducos-Galand, M., Bland, M.J., and Mazel, D. (2012). Genome engineering in *Vibrio cholerae*: a feasible approach to address biological issues. PLoS Genet. *8*, e1002472.
35. Kovach, M.E., Elzer, P.H., Hill, D.S., Robertson, G.T., Farris, M.A., Roop, R.M., 2nd, and Peterson, K.M. (1995). Four new derivatives of the broad-host-range cloning vector pBBR1MCS, carrying different antibiotic-resistance cassettes. Gene *166*, 175–176.
36. Zhang, Y., Deng, Y., Feng, J., Guo, Z., Chen, H., Wang, B., Hu, J., Lin, Z., and Su, Y. (2021). Functional characterization of VscCD, an important component of the type III secretion system of *Vibrio harveyi*. Microb. Pathog. *157*, 104965.
37. Zhao, X., Cui, Y., Yan, Y., Du, Z., Tan, Y., Yang, H., Bi, Y., Zhang, P., Zhou, L., Zhou, D., et al. (2013). Outer membrane proteins ail and OmpF of *Yersinia pestis* are involved in the adsorption of T7-related bacteriophage Yepphi. J. Virol. *87*, 12260–12269.
38. Lin, Y.R., Chiu, C.W., Chang, F.Y., and Lin, C.S. (2012). Characterization of a new phage, termed ϕA318, which is specific for *Vibrio alginolyticus*. Arch. Virol. *157*, 917–926.
39. Zhao, Z., Chen, C., Hu, C.Q., Ren, C.H., Zhao, J.J., Zhang, L.P., Jiang, X., Luo, P., and Wang, Q.B. (2010). The type III secretion system of *Vibrio alginolyticus* induces rapid apoptosis, cell rounding and osmotic lysis of fish cells. Microbiology (Read.) *156*, 2864–2872.
40. Kiljunen, S., Datta, N., Dentovskaya, S.V., Anisimov, A.P., Knirel, Y.A., Bengoechea, J.A., Holst, O., and Skurnik, M. (2011). Identification of the lipopolysaccharide core of *Yersinia pestis* and *Yersinia pseudotuberculosis* as the receptor for bacteriophage ϕA1122. J. Bacteriol. *193*, 4963–4972.
41. Wang, T., Yao, L., Qu, M., Wang, L., Li, F., Tan, Z., Wang, P., and Jiang, Y. (2022). Whole genome sequencing and antimicrobial resistance analysis of *Vibrio parahaemolyticus* Vp2015094 carrying an antimicrobial-resistant plasmid. J. Glob. Antimicrob. Resist. *30*, 47–49.
42. Chen, S., Zhou, Y., Chen, Y., and Gu, J. (2018). fastp: an ultra-fast all-in-one FASTQ preprocessor. Bioinformatics *34*, i884–i890.
43. Delcher, A.L., Phillippy, A., Carlton, J., and Salzberg, S.L. (2002). Fast algorithms for large-scale genome alignment and comparison. Nucleic Acids Res. *30*, 2478–2483.
44. Schwartz, S., Kent, W.J., Smit, A., Zhang, Z., Baertsch, R., Hardison, R.C., Haussler, D., and Miller, W. (2003). Human-mouse alignments with BLASTZ. Genome Res. *13*, 103–107.
45. Li, H., and Durbin, R. (2009). Fast and accurate short read alignment with Burrows-Wheeler transform. Bioinformatics *25*, 1754–1760.
46. Mellitzer, A., Glieder, A., Weis, R., Reisinger, C., and Flicker, K. (2012). Sensitive high-throughput screening for the detection of reducing sugars. Biotechnol. J. *7*, 155–162.

STAR★METHODS

KEY RESOURCES TABLE

REAGENT or RESOURCE	SOURCE	IDENTIFIER
Bacterial and virus strains		
E. coli SM10 λpir	Jiao Lab	CAS: ZC1038
E. coli GEB883	Deng Lab	Nguyen et al.[32]
E. coli DH5a	Vazyme	CAS: 9057
E. coli BL21(DE3)	Vazyme	CAS: 9126
E. coli S17-1λpir	This Lab	Milton et al.[33]
V. alginolyticus E110	This Lab	GenBank no. PRJNA842900
V. alginolyticus EP1-5	This Lab	GenBank no. PRJNA1009694
pSW7848	Deng Lab	Val et al.[34]
pBBR1MCS-1	Deng Lab	Kovach et al.[35]
pCold-TF	Takara	CAS: 3365
Biological samples		
Seawater	Guangzhou	N/A
Chemicals, peptides, and recombinant proteins		
2, 6-Diaminopimelic acid	Merck Millipore	CAS: 583-93-7
Chloramphenicol	Merck Millipore	CAS: 56-75-7
Kanamycin	Sangon Biotech	CAS: 25389-94-0
Ampicillin	Sangon Biotech	CAS: 69-52-3
D-glucose	Merck Millipore	CAS: 50-99-7
L-arabinose	Merck Millipore	CAS: 5328-37-0
Ethylenediaminetetraacetic acid	Merck Millipore	CAS: 60-00-4
3-sulfopropyltetradecyldimethylbetaine	Sangon Biotech	CAS: 14933-08-5
hydrochloric acid	Merck Millipore	CAS: 7647-01-0
Ammonium sulfamate	Merck Millipore	CAS: 7773-06-0
Sodium tetraborate	Merck Millipore	CAS: 1330-43-4
3-hydroxyldiphenol	Merck Millipore	CAS: 580-51-8
Glucuronic acid	Merck Millipore	CAS: 6556-12-3
Proteinase K	Merck Millipore	CAS: 39450-01-6
Isopropyl-*β*-d-thiogalactopyranoside	Merck Millipore	CAS No.: CAS: 367-93-1
BugBuster® Master Mix	Merck Millipore	CAS: 70584-M
Ni-NTA Agarose	Qiagen	CAS: 30210
Paraformaldehyde	Merck Millipore	CAS: 30525-89-4
HIS antibody	Cell Signaling Technology	RRID: AB_10786151
Alexa Fluor® 594 goat anti-rabbit IgG	Cell Signaling Technology	RRID: AB_2650602
Critical commercial assays		
FastPure Bacteria DNA Isolation Mini Kit	Vazyme	DC112-01
Capsular stain kit	Solarbio	G1130-50
BCA protein assay kit	Biosharp	PC0020
Deposited data		
NCBI database	The genome sequence	https://www.ncbi.nlm.nih.gov/genome/

(*Continued on next page*)

Continued

REAGENT or RESOURCE	SOURCE	IDENTIFIER
Oligonucleotides		
Primers for identification of phage bacterial receptors, see Tables S4 and S5	This paper	N/A
Primers for identification of phage receptor-binding proteins, see Table S6	This paper	N/A
Software and algorithms		
Structural domains	Web	https://www.ebi.ac.uk/interpro/

RESOURCE AVAILABILITY

Lead contact

Further information and requests for resources and reagents should be directed to and will be fulfilled by the lead contact, Zhe Zhao (zhezhao@hhu.edu.cn).

Materials availability

All unique/stable reagents in this study are available from the lead contact without restriction.

Data and code availability

- The whole genome sequence for *V. alginolyticus* E110 obtained through the Illumina Miseq platform was deposited in GenBank under BioProject number PRJNA842900. The genome sequence-associated data for five spontaneous HH109-resistant mutants were deposited in GenBank under BioProject number PRJNA1009694. These data are publicly available as of the date of publication.
- This paper does not report the original code.
- Additional information required to reanalyze the data in this paper is available from the lead contact upon request.

EXPERIMENTAL MODEL AND STUDY PARTICIPANT DETAILS

No experimental models were used in this study.

METHOD DETAILS

Bacterial strains, plasmids, and growth conditions

The bacterial strains and plasmids used in this study are summarized in Tables S1, S2, and S3. *V. alginolyticus* strains were cultured at 37°C in Luria-Bertani (LB, Huankai, China) broth supplemented with 2% NaCl or Thiosulfate-Citrate-Bile Salts-sucrose-agar (TCBS, Huankai, China). *E. coli* strains were cultured in LB broth or agar plate at 37°C. *E. coli* SM10 strain bearing the plasmid pSC189 was used to construct the transposon mutation library of the *V. alginolyticus* E110 strain. *E. coli* GEB883 growth was cultured in an LB medium with 50 μg/mL DAP (2, 6-Diaminopimelic acid) and used for conjugation in gene deletion experiments. Suicide plasmid pSW7848 was used to generate gene deletion mutants in *V. alginolyticus* strains, and the low-copy vector pBBR1MCS-1 was used for complementation experiments. pCold-TF vector was used for the protein expression of gp02. Unless otherwise specified, Antibiotics were used at the following concentrations: Chloramphenicol (Cm), 25 mg/mL; Kanamycin (Kan), 100 mg/mL; Ampicillin (Amp), 100 mg/mL.

Transposon mutagenesis and screening of phage-resistant mutants

To create a random mutant library, donor bacterial strain SM10 containing transposon pSC189 was conjugated with recipient strain E110 on LB at a 1:1 donor-to-recipient ratio. After culture overnight, 100 μL of the transformed bacterial suspension was streaked on TCBS plates containing 100 μg/mL kanamycin and incubated at 30°C overnight. Subsequently, individual colonies were picked into 96-deep-well plates and cultured for 6-8 h in 600 μL LB broth with 2% NaCl per well supplemented with 60 μg/mL Kan. The resulting mutant pool was then stored at -80°C. The pool consists of 30,760 mutants in 321 microplates and represents sixfold coverage of the genome (i.e., averages 6 insertions per gene) with greater than 99% assurance of covering the entire genome.

To screen phage-resistant mutants, two rounds of screening were performed as described previously with a slight modification.[5] For the first round, each mutant with approximately 10^8 CFU/mL was infected with the phage HH109 at an MOI of 1 in a 96-well plate and incubated at 37°C, shaking at 120 rpm for 4 h. As a control, the wild-type E110 was also included as performed under the same conditions. Then, the turbidity (OD_{600}) for each well was quantified using a Microplate reader (SPARK; Tecan). For the second round, suspected phage-resistant colonies obtained from the first screening were further confirmed using spot testing. In brief, after the 20 μL bacterial suspensions (~10^8 CFU/mL) were air-dried on an LB agar plate containing 2% NaCl, 3 μL phage (10^8 PFU/mL) was added to the center of the bacterial lawn and then cultured at 37°C for 4 h. In principle, the phage HH109 can cause a clearing of the bacteria encompassing the original spot in the wild-type strain, whereas not in phage non-susceptible mutants.

Transposon insertion site determination

Tail-PCR products determined the transposon-insertion site of these 11 phage HH109-resistant mutants. Genomic DNA from the stored phage HH109-resistant mutants were isolated using a FastPure Bacteria DNA Isolation Mini Kit (Vazyme, China) per manufacturer instructions. All primers used in this section are listed in Tables S4 and S5. After a round of PCR amplification using the mutant strain DNA, the PCR product used for the second round of PCR is used as the template. The PCR products were sequenced (Sangon Biotechnology, China) and performed to BLAST in the NCBI database to determine the transposon insertion site.

Gene knockout and complementation

All gene deletion strains were generated using homologous recombination, as described previously.[36] Briefly, the upstream and downstream arms of the target gene were amplified by PCR using indicated primers (Tables S4 and S5), and the two arms were then used as the templates to generate a gene deletion fragment, which was then cloned into the suicide vector pSW7848. PCR amplified the vector fragment pSW7848 with the primer pair pSW7848-F/R (Table S4). The recombinant suicide plasmids were obtained by isothermal assembly and transformed into DAP-auxotrophic *E. coli* GEB883 cells. The positive colonies were detected on LB plates containing Cm 25 and 50 μg/mL DAP using the primers annotated Del-check-pSW7848-F/R. Then, the recombinant suicide plasmid was transferred by conjugation from strain GEB883 to *V. alginolyticus* wild-type strain E110 before allelic exchange. Transconjugants were first selected on TCBS plates containing 0.2% D-glucose and 5 μg/mL chloramphenicol and then selected on TCBS plates containing 0.2% L-arabinose to induce the suicide *ccdB* gene expression. The deletion of genes was confirmed by PCR (Tables S4 and S5).

The complete open reading frame with the promoter region of each indicated target gene was PCR-amplified for complementation experiments using primers containing cut sites for EcoRI (forward) and SalI (reverse) restriction enzymes and cloned into the pBBR1MCS-1 vector. As described above, the recombinant plasmids were transformed into the corresponding knockout mutants by conjugation using *E. coli* S17-1λpir as the donor strain. The transformed colonies were screened on TCBS plates supplemented with 5 μg/mL chloramphenicol and confirmed via PCR. The primers used in this part are listed in Tables S4 and S5.

Lysis curve determination and spot testing assays

Growth kinetics of wild-type, deletion mutants, and complemented strains were determined using the Bioscreen C (FP-1100-C, Bioscreen), measuring the turbidity OD_{600} every 1 h interval with an MOI of 1. Spot testing was performed as described above. A small volume of HH109-containing diluent (10-fold serial dilutions) was added onto the dried bacterial lawn of the indicated strains on an LB agar plate with 2% NaCl. After 4 h of incubation at 37°C, clear zones were recorded to reflect the inhibition of bacterial growth.

Phage adsorption assay

The adsorption capacities of the phage HH109 on the wild-type, deletion mutants, and complemented strains were conducted as described previously with slight modifications.[37] Briefly, bacterial cells with a 10^6 CFU/mL density were infected with the phage at an MOI of 0.01. The mixtures were incubated at 37°C for 10 min and then immediately centrifuged at 10000 g at 4°C for 1 min to pellet bacterial cells. Subsequently, free phage particles in the supernatant were quantified by the double-layer agar method to calculate the phage adsorption rate.[38]

Microscopy observation on the bacterial capsule

To observe the cell surface structure of the wild-type, deletion mutants, and complemented strains, scanning electron microscopy (SEM) was first used, and all samples were prepared as described previously.[39] Briefly, these strains were cultured overnight at 37°C and then fixed in 2.5% glutaraldehyde for 2 h at room temperature (RT). After being washed three times with 0.1 M PBS (pH 7.4), they were treated with 1% osmium tetroxide in 0.1 M PBS (pH 7.4) for 2 h at RT, followed by dehydration with sequential washes in 30, 50, 70, 80, 95 and 100% ethanol and dry using a critical-point dryer (K850, Quorum). All samples were coated with gold using an ion sputter coater (MC1000, Hitachi) and observed under a scanning electron microscope (SU8100, Hitachi).

For further qualitative observation of capsules in those strains, capsule staining was performed using a capsular stain kit according to the manufacturer's instructions (Solarbio, China). Concisely, a drop of bacterial suspension was smeared on a clean glass slide. After drying, the slide was flooded with crystal violet solution for 5 min, rinsed with copper sulfate solution, and blotted dry with filter paper. Slides were examined using light microscopy under oil immersion (Axio Vert.A1, Carl Zeiss).

Capsule extraction and quantification

For quantitative analysis of CPS in various *V. alginolyticus* strains, as indicated, extraction and quantification of surface CPS were performed. The 500 mL cultures of *V. alginolyticus* were grown in LB broth containing 2% NaCl at 37°C until the OD_{600} reached 0.8. The cells were then harvested by centrifugation (8000 g, 5 min, at 4°C) and washed with 100 mL of sterile saline solution (2% NaCl). After that, the cells were pelleted again (8000 g, 5 min, at 4°C) and resuspended in 100 mL of 50 mM EDTA (pH 8.0). The sample was incubated at 30°C for 1 h, and the precipitate was washed with 100 mL of sterile saline solution (2% NaCl). The washed precipitate was collected by centrifugation (8000 g, 5 min, at 4°C) and resuspended in 100 mL of sterile saline solution (2% NaCl) to which 20 mL of 1% 3-sulfopropyltetradecyldimethylbetaine (pH 2.0) was added. After mixing, the sample was heated at 50°C for 30 min and then centrifuged at 8000 g for 5 min at 4°C. The resulting supernatant (120 mL) was mixed with a chloroform-n-butanol mixture (5:1, 24 mL) by inverting and allowed to stand for 30 min at RT. The mixture was then

centrifuged at 8000 g for 5 min at 4°C. The uppermost aqueous phase containing CPS was precipitated with four times the volume of cold 100% ethanol by inverting and incubated at 4°C for 12 h. The samples were pelleted by centrifugation (12,000 g, 10 min, at 4°C), washed with 70% ethanol, and lyophilized using the vacuum freeze dryer (Alpha-2LDPLUS, Christ).

The purified CPS dry powder was reconstituted in 250 μL of 100 mM hydrochloric acid, and 100 μL of CPS solution was added to 5 μL of pre-cooled 4 M ammonium sulfamate and 600 μL of 25 mM sodium tetraborate. The mixture was vortexed vigorously and boiled for 15 min. After cooling to RT, 40 μL of 0.15% 3-hydroxyldiphenol was added, and the samples were aliquoted to a 96-well plate. The absorbance was measured at 520 nm, and standard curves were determined using 100 μL of glucuronic acid (0 to 40 μg/mL).

Identification of the phage receptor type

The receptor properties of HH109 were measured as described previously.[40] Briefly, exponentially growing *V. alginolyticus* were treated with proteinase K (0.2 mg/mL; Qiagen) to destroy surface proteins at 37°C for 2 h. After that, the treated bacteria were washed thrice with fresh LB broth with 2% NaCl. Adsorption assays were performed for the various treated cells using double-layer agar plate assays.

Isolation of phage-resistant *V. alginolyticus* mutants

As performed in the spot testing assay above, 30 μL of the phage HH109 (approximately 10^5 PFU/mL in phage titer) were spotted onto bacterial lawns and incubated at 37°C overnight. When bacterial colonies regrew in the middle of lysis zones, several of them were randomly picked from different spots. These colonies were then streaked on LB agar plates containing 2% NaCl for purification by three rounds of single colony isolation, and the phage-resistant phenotypes were further confirmed by spot testing and growth curve assays.

Genome sequencing and comparative analysis

The whole-genome sequencing of the wild-type *V. alginolyticus* was performed using the Pacific Biosciences platform (PacBio, Menlo Park, CA) and the Illumina Miseq platform. According to the manufacturer's instructions, the total DNA of *V. alginolyticus* E110 was extracted using the HiPure Bacterial DNA kit (Magen, Guangzhou, China). The quality of the extracted DNA was determined using Qubit (Thermo Fisher Scientific, Waltham, MA) and Nanodrop (Thermo Fisher Scientific, Waltham, MA). The library construction and data analysis were completed by Gene Denovo (Guangzhou, China), and the detailed information refers to previous reports.[41] The genome of five spontaneous HH109-resistant mutants and sixteen naturally occurring phage-resistant strains of *V. alginolyticus* were sequenced using a Novaseq 6000 owned by Guangzhou Gene Denovo Co., Ltd. Coding sequences (CDSs) in each draft genome were predicted using Prodigal 2.60 with the default settings. High-quality reads were filtered and obtained using FASTP (version: 0.20.0).[42] Coverage of the *V. alginolyticus* genome was evaluated using SOAPaligner (http://soap.genomics.org.cn/soapaligner.html), and reads were assembled using SOAPdenovo (http://soap.genomics.org.cn/soapnovo.html). Afterward, SNP mutations were obtained after sequence alignment using the software package MUMmer (version 3.23).[43] The initial InDels (less than 10 bp) were obtained for alignment using LASTZ and axtBest.[44] Reliable InDel sites were obtained using BWA software[45] to align the 150 bp (3sd) upstream and downstream of the reference sequence InDel sites and verified by sample sequencing. BLASTp was also used to explore the variation in phage-resistant strains, which was conducted by aligning the Nucleic acid sequence of our strains to the reference genome E110 (CP098035.1).

Protein expression, purification, and anti-serum preparation

A large fragment of *gp02* (covering C-terminal sequence from 1072 bp to 2820 bp) was amplified from the genome of phage HH109 using the primers pCold-TF-F/R (Table S6) and cloned into the pCold-TF vector (Takara, Japan) using One Step Cloning Kit (Vazyme, China) to generate the recombinant plasmid pCold-TF/*gp02*. The construct was transformed into *E. coli* BL21(λDE3) plysS cells and the bacteria were then induced with 0.6 mM isopropyl-*β*-d-thiogalactopyranoside (IPTG) at 20°C for 24 h to express the recombinant protein gp02, which contained the tag proteins Trigger factor (TF) and 6× His. The induced cultures were harvested by centrifugation and resuspended in BugBuster® Master Mix (Millipore, USA) following manufacturer protocol to achieve cell lysis. The supernatant of cell lysates mixed with Ni-NTA Agarose (Qiagen, Germany) was incubated overnight at 4°C with gentle agitation. The mixture containing the recombinant protein was then loaded onto a column and purified using Ni-NTA affinity chromatography. The recovery and purity of protein in each fraction were checked by sodium dodecyl sulfate-polyacrylamide gel electrophoresis (SDS-PAGE) and pooled. The protein concentration was estimated by using a BCA protein assay kit (Biosharp, China). As a control, empty vector pCold-TF was simultaneously performed following the same procedure as the pCold-TF/*gp02*. Anti-gp02 serum was obtained by immunizing New Zealand white rabbits with the purified recombinant protein gp02-TF (ABclonal, China).

Antibody blocking and protein competition assay

For antibody blocking assay, 200 μL anti-gp02 serum and normal serum were individually mixed with the phage HH109 at a concentration of 10^5 PFU/mL for 10 min at RT, and *V. alginolyticus* strain E110 was then added into the mixture to allow phage infection for 1 h, and the phage titer of HH109 was determined by the double-layer agar method. For protein competition assay, 2 mg/mL of the purified gp02-TF was incubated with an equal volume of E110 at a cell density of 10^8 CFU/mL for 10 min at RT. As a control, the tag protein TF produced from the pCold-TF vector was included to do the same thing. Then, 10^6 PFU/mL of phage HH109 was added to the above mixtures to calculate the adsorption rate.

Immunofluorescence analysis

To detect the binding of gp02 to host CPS, immunofluorescence staining was carried out using the anti-gp02 serum. Overnight, the wild-type strain or Δ*ugd* strain was pre-incubated with equal volume of the purified gp02-TF (2 mg/mL) for 30 min at RT and pelleted by centrifugation. These strains were washed three times with sterile saline solution (2%NaCl) and fixed in 4% paraformaldehyde (Merck, Germany) for 15 min at RT. After blocking in 10% normal goat serum for 1 h, bacterial cells were incubated with the HIS antibody (1:500; Cell Signaling Technology, USA) in 1% normal goat serum for 2 h at RT, rinsed three times for 10 min each with sterile saline solution (2% NaCl), and then incubated with the Alexa Fluor® 594 goat anti-rabbit IgG (1:500; Cell Signaling Technology, USA) for 1 h at RT in the dark. Bacterial cells were then smeared onto a glass slide and examined under a fluorescence microscope (Axio Vert.A1, ZEISS). The tagged protein TF was also included to incubate with the wild-type strain as a negative control similarly.

Assays on degradation activity of purified gp02

The degradation activity of purified gp02 was demonstrated using several qualitative and quantitative experiments. Firstly, the wild-type E110 strain was pre-treated with 500 ng of the purified gp02 or TF at RT for 15 min or untreated and then subjected to capsule staining and CPS quantification. Capsule staining was performed as described above, and stained cells were observed under light microscopy. Extraction and quantification of CPS were also carried out following the above protocol, and the Δ*ugd*, a capsule-deficient strain, was included in this assay as a negative control. Next, to visualize CPS degradation, aliquots of purified CPS (50 μg) were incubated with an equivalent volume of two-fold serial diluted gp02 (500 ng-62.5 ng) or 500 ng TF at RT for 1 h. Then, all samples were separated by 6-12% gradient SDS-PAGE and stained with Alcian Blue.[46] Briefly, the gel was washed in fixing solution (25% ethanol and 10% acetic acid in Milli-Q water) at 50°C for 15 min and stained with 0.125% Alcian blue in fixing buffer for 20 min at 50°C in the dark. Consequently, the gel was detained in fixing buffer overnight at RT and visualized.

Assay of biofilm-dispersing activity

To evaluate the biofilm degradation efficacy of phage HH109, 1% of an overnight bacterial culture was inoculated into HI fresh broth containing 0.8% NaCl and cultured on 24-well-polystyrene plates for 12 h (n = 6) at 30°C. The biofilms were washed to remove the residual planktonic bacterial cells, and the phage with concentrations 1.2×10^9, 1.2×10^8, and 1.2×10^7 pfu/mL were treated for 2, 4, 6, and 8 h. Then, the supernatant was removed from the well and washed twice. The total biomass was quantified using a crystal violet staining assay.

QUANTIFICATION AND STATISTICAL ANALYSIS

All data are presented as means ± the standard deviations(s.d.) from a minimum of three independent experiments. Statistical analysis was carried out using Student *t* tests or two-way ANOVA using GraphPad Prism v7 software. $P \leq 0.05$ was considered significant. Significance is indicated in the figures by asterisks (*, $P \leq 0.05$; **, $P \leq 0.01$; ****, $P \leq 0.0001$).

ADDITIONAL RESOURCES

No additional resources are involved.